Experimental investigations into thermal performance of phase change emulsion in a fin-and-tube heat exchanger

Cai Wei[1,†], Jingjing Shao[1,*,‡] and Jo Darkwa[2]

[1]*Department of Civil and Transportation Engineering, Ningbo University of Technology, Ningbo 215040, China;* [2]*Architecture, Climate and Environment Research Group, Faculty of Engineering, University of Nottingham, University Park, NG7 2RD Nottingham, UK*

Abstract

Phase change emulsions (PCMEs) are always identified as potential working fluids that could be used to reduce circulating pump energy consumption in chill water air conditioning systems. But how PCME behaves in a fin-and-tube heat exchanger is still unclear, which limited the application of such material. The paper focused on experimental studies of performance of a novel PCME, named as PCE-10, in a fin-and-tube heat exchanger. The research analyzed heat transfer and flow behavior in fin-and-tube heat exchangers and the experimental results are compared with numerical studies published. Both studies showed that PCE-10 had its advantages as a cold storage medium, as PCE-10 did help to improve the heat transfer rate of heat exchanger by factor of 1.1–1.3 at the same flow rate compared with water.

Keywords: experimental study; flow behavior; heat transfer; fin-and-tube heat exchanger; phase change emulsion

*Corresponding author:
jingjing.shao@nbut.edu.cn

Received 6 September 2022; revised 23 November 2022

1 INTRODUCTION

Chilled-water air conditioning systems are used widely in large-scale air-conditioning projects around the world, and they are still gaining popularity due to climate changes. Among all the components inside the system, chilled water circulating pumps is a major energy consumer that is responsible for ∼15%–30% of the system's energy consumption [1, 2]. Energy consumption of pump is highly related to amount of fluid transmitted. So if the heat storage capacity of chilled water could be increased, the volume of chilled water required to deliver the same amount of heat can be cut and thus achieves the aim of energy saving. That is when researchers started to add phase change materials (PCMs) such as paraffin into water, forming PCM emulsions (PCMEs) [3–5]. PCMEs make uses of the latent heat of paraffin, as well as sensible heat of water and that of the PCM to store thermal energy. PCMEs do not lose the fluidity during phase transition. Hence, they can be directly used both in storage systems and in pumped systems like chilled-water air conditioning system.

Researchers have already developed several different types of PCME suitable for comfort cooling application, for instance, tetradecane emulsion [6], hexadecane emulsions [7] and RT10 emulsion [8]. Several studies on the thermophysical properties [9–12] flow characteristics [13, 14] and heat transfer performance [10, 15–19] of PCMEs have been performed, confirming the fluidity and heat transfer benefits of the PCMEs. Even though there are some reports on PCMEs' behavior in rectangular enclosures [19], air-emulsion direct-contact heat exchanger [20], double-coiled heat exchanger [21, 22], investigations on heat transfer characteristics in fin-and-tube heat exchangers appear to be limited for practical engineering so far.

In an effort to understand the heat transfer effectiveness and fluid characteristics of PCMEs, an experimental setup consisting of a fin-and-tube heat exchanger was designed for that purpose. These results will be used to validate the test results with the numerical predictions from [23].

2 PHASE CHANGE MATERIAL EMULSION

In order to study the thermal performance, a stable and suitable paraffin/water PCME (PCE-10) was developed based on a

† Cai Wei[1], https://orcid.org/0000-0002-7296-3936
‡ Jingjing Shao[1,*], https://orcid.org/0000-0003-3497-7330

International Journal of Low-Carbon Technologies 2023, 18, 175–183

https://doi.org/10.1093/ijlct/ctad001 Advance Access publication 24 March 2023

Figure 1. *Developed PCME sample PCE-10 based on [8].*

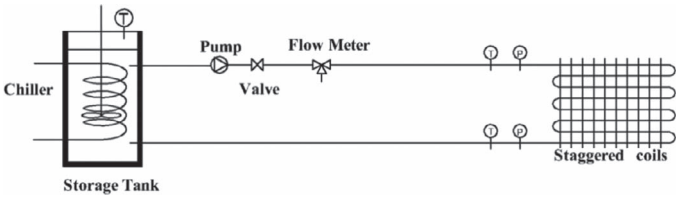

Figure 2. *Scheme of the test rig.*

commercialized material called RT10. The detailed preparation procedure can be found in [8]. The final product is shown in Figure 1. The developed PCE-10 has a phase change temperature range of 4°C–11°C falling into the temperature range of chilled water air conditioning system and is an attractive candidate for cooling applications.

3 EXPERIMENTAL SETUP

An experimental setup for the determination of the pressure drop and heat transfer performance of a commercially available fin-and-tube heat exchanger using PCE-10 as a coolant was built. The schematic view of the test rig is shown in Figure 2. The PCE-10 was stored at 7°C in an insulated thermostatic bath equipped with cooling device. The fin-and-tube heat exchanger was manufactured by Xinhong Refrigeration Co., Ltd as detailed in Figure 3 and Table 1. The coolant was distributed into the coil from the inlet manifold located on the top of the coil and returned to the storage tank through the bottom outlet.

The volume flow rate of the PCE-10 was measured at the inlet of finned-tube coil with an accuracy of ±0.1%. The temperatures of fluid and air flow, as well as the tube wall temperature were measured at the coil inlet and outlet by K-type thermocouples with accuracy of ±0.07%. The pressure drop was measured by two pressure sensors with accuracy of ±1%. The air velocity was

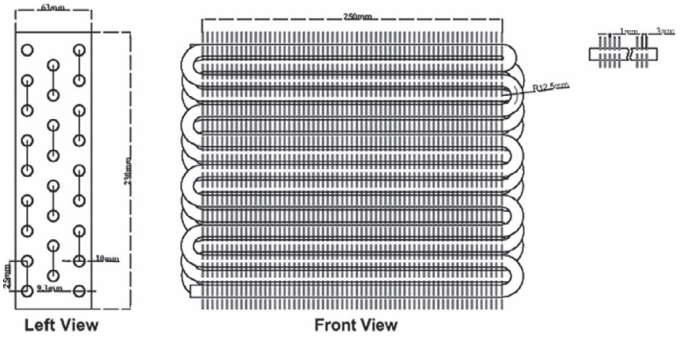

Figure 3. *Geometry of finned-tube coil.*

measured at the inlet and outlet flow cross-sections with TESTO anemometer 410-1, whose accuracy is ±2%. The full specifications are presented in Table 2. Before experiments, anemometer, thermocouples and pressure sensors were calibrated by comparing the device for calibration to other devices with a proven accuracy. As to the rotameter, it was calibrated with water and PCE-10 separately. The liquid was pumped through rotameter at a certain controlled flow rate; then, the readings of rotameter were compared with the flow rate supplied.

4 EXPERIMENTAL PROCEDURE

Different sets of experiments were conducted to determine the pressure drop and heat transfer performance of developed PCE-10 in fan-coils units. Initial experiments were carried out with water, and the results are served as control groups.

The pressure drops of PCE-10 were measured under almost isothermal conditions (fan turned off) and inlet temperature at 10°C. The flow rate used here varied between 40 and 144 L/h at intervals of 8 L/h.

The heat transfer experimental analysis was carried out under standard operation conditions. In chilled water fan coil unit systems, the optimal chilled water flow and air velocities are 0.3–0.5 and 1.5–2 m/s [24, 25]. Therefore, the following operating conditions were adopted: flow rate of 40–120 L/h, inlet air temperature of 27°C, air flow velocity of 0.8, 1 and 1.5 m/s.

5 DATA DEDUCTION

To describe the flow inside the tube, the generalized Reynolds number (Re) needs to be introduced:

$$\mathrm{Re}^* = 8^{1-n}\left(\frac{3n+1^{-n}}{4n}\right)\frac{\rho u^{2-n}D_i^n}{\delta} \tag{1}$$

$$Nu = \frac{hD_i}{\lambda}, \tag{2}$$

Table 1. *Fin-and-tube coil data.*

Symbols		Dimension	Symbols		Dimension
P_f	Twice the amplitude of fins corrugation	3 mm	$\mathbf{K_{fin}}$	Conductivity of fin	200 W/mK
N_{bank}	Number of banks of tubes	3	$\mathbf{x_f}$	Half wavelength of in wave	1.5 mm
$N_{tubes/bank}$	Number of tubes per bank	9	**D**	Interior diameter of tube	9.3 mm
N_{fin}	Number of fins	83	**r**	Outer radius of tube	4.96 mm
N_{fin}	Number of fins	83	$\mathbf{A_f}$	Total wetted area of fins	$2.3m^2$
P_t	Transverse pitch	25 mm	$\mathbf{A_{a,total}}$	Total airside area	$2.8m^2$
P_l	Longitudinal bank-bank pitch	22 mm	$\mathbf{A_{tube}}$	Total outer area of tubes	$0.21m^2$
L_{tube}	Length of one tube	0.25 m	$\mathbf{D_{coil}}$	Diameter of turning	25 mm

Table 2. *Rig specification.*

Data loggers and sensors:
Agilent Technologies-Data Logger Switch Unit 34970A Data Acquisition
LZB-10 glass rotameter flow meter Accuracy: ±2.5%
TESTO- Anemometer 410–1 Accuracy: ±(0.2 m/s + 2% of reading)
SZ Joint Sensor Instruments (H.K.) Ltd - Model 641S Pressure Sensor Accuracy: ±1%
Omega-K type thermocouple Accuracy: ±0.07%.
Cooling units:
Tianheng Instrument Factory-Low-Temperature Thermostat Bath THD-1010
Cooling medium temperature: 7 °C
Flow rate: 160 L/h to 40 L/h
Coil:
Xinhong Refrigeration Co., Ltd-Fin-and-Tube Coil (3-Row)

where *n* characterizes the degree of non-Newtonian behavior of fluids. As stated earlier, the PCE-10 is a non-Newtonian fluid and so *n* equals to 0.51 in this case. For water that is a Newtonian fluid, $n = 1$.

As the tube wall temperature is difficult to measure for finned surface, the fluid side heat transfer coefficient is calculated through overall heat transfer coefficient and air-side heat transfer coefficient.

The heat transfer rate (Q) of heat exchanger was determined from the energy balances on the fluid side and on the air side. The air-side heat transfer rate and fluid-side heat transfer rate, which are calculated as

$$Q_{air} = C_{p,air} \times m_{air} \times T_{air,diff} + m_{air} \times LH \times \left(g_{in} - g_{out}\right) \quad (3)$$

$$Q_{fluid} = C_{p,fluid} \times m\,fluid \times T\,fluid, diff \quad (4)$$

where

LH = latent heat of vaporization of water = 2450 kJ/kg;

g_{in}-g_{out} = air moisture content difference (kg/kg).

The air temperature and relative humidity at the inlet and outlet cross-sections were determined by averaging the experimental measurements. The air mass flow rate was obtained by considering the outlet air density.

A detailed analysis of the experimental uncertainties was carried out. The uncertainty calculation procedure was based on the application of the general uncertainty propagation expression according to the ISO Guide [26] to the calculated magnitudes. The uncertainty analysis revealed that the mean typical uncertainties in the calculation of the heat transfer rate from the energy balance on the air side are higher than from the energy balance on the fluid side. The mean values of the mean typical uncertainties in the heat transfer rate from the energy balance on the fluid side and on the air side were 5.8% and 30.8%, respectively. Taking into account these results, the capacity of the fan-coil was calculated at the fluid side.

The relationship between the overall heat transfer coefficient (U) and the heat transfer rate (Q) can be demonstrated by the following equation:

$$Q_{fluid} = U \times A \times T_m = U \times (\pi\ D_i L) \times F \times LMTD. \quad (5)$$

T_m, also named as logarithmic mean temperature difference (LMTD) for a counter-current heat exchanger, was defined as

$$LMTD = \frac{\left(T_{H,out} - T_{C,in}\right) - \left(T_{H,in} - T_{C,out}\right)}{\ln\left[\left(T_{H,out} - T_{C,in}\right) / \left(T_{H,in} - T_{C,out}\right)\right]}. \quad (6)$$

The LMTD correction factor F is required because the heat exchanger is cross-flow rather than parallel-flow or counter-flow. The correction factor is obtained from the calculation of two ratios P and R associated with the inlet and outlet temperatures of the two fluids as shown in Yao's study [27].

Table 3. *Measured pressure drop at different flow rates for PCE-10 and water.*

		Flow Rate (L/h)						
		24	**32**	**40**	**48**	**56**	**64**	**72**
Pressure drop (kPa)	Water	2.40	2.40	2.41	2.43	2.43	2.43	2.45
	PCE-10	15.5	16.46	18.04	19.41	21.39	24.05	27.63
		80	**88**	**96**	**104**	**112**	**120**	
Pressure drop (kPa)	Water	2.57	3.07	3.53	4.05	4.65	5.28	
	PCE-10	32.11	35.09	37.00	38.29	41.01	43.15	

Several equations can be used to determine the liquid side heat transfer coefficient value h_{fluid}; one of which is shown in Equation (7). As the wall thickness of the tube is small and the thermal conductivity of the tube material is high, the thermal resistance of the tube is negligible, so it is ignored for later calculation ($R_{wall} = 0$).

$$\begin{aligned}\frac{1}{U\times A} &= \frac{1}{h_{fluid}\times A_{fluid}} + R_{\text{wall}} + \frac{1}{(\eta^*\times h_{air}\times A_{air})} \\ &= \frac{1}{h_{fluid}\times A_{fluid}} + \frac{\ln(D_{ext}/D_{\text{int}})}{k\times 2\,\pi L} + \frac{1}{(\eta^*\times h_{air}\times A_{air})} \\ &\approx \frac{1}{h_{fluid}\times A_{fluid}} + \frac{1}{(\eta^*\times h_{air}\times A_{air})}\end{aligned}, \tag{7}$$

where $\eta*$ is the surface efficiency defined by Schmidt [27].

$$\eta^* = 1 - \frac{A_f}{A_{a,total}}\left(1-\eta_f\right) \tag{8}$$

$$\phi = \left(\frac{r_f}{r}-1\right)\left[1+0.35\ln\left(\frac{r_f}{r}\right)\right] \tag{9}$$

$$\eta_f = \frac{\tanh\left(mr\phi\right)}{mr\phi} \tag{10}$$

$$m = \sqrt{\frac{2h_a\left(\frac{C_s}{C_p}\right)}{k_{fin}t}}, \tag{11}$$

where

r = outer diameter of tube;

r_f = the outer radius of fin;

C_s/C_p = the correction for heat/mass transfer for a wetted surface. C_s/C_p is set to unity if the fins are dry.

In order to determine the heat transfer coefficients between the fluids and the heat exchanger surface, convection correlations must be used. The air side heat transfer coefficient for wavy-louvered fins is calculated from following empirical overall correlations [26].

$$j = 16.06\text{Re}_D^{-1.02(pf/D)-0.256}\left(\frac{A_{a,total}}{A_{tube}}\right)^{-0.601} N_{bank}^{-0.069}\left(\frac{pf}{D}\right)^{0.84} \tag{12}$$

$$h_{air} = \frac{j\rho\left(m_{air}/\rho A_c\right)C_p}{\text{Pr}^{2/3}} \tag{13}$$

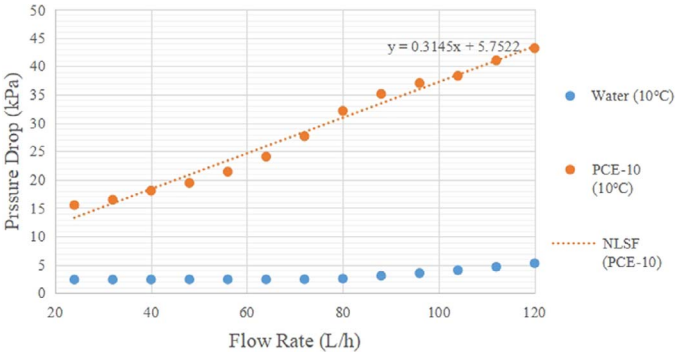

Figure 4. *Pressure drop of PCME vs water at 10°C.*

Recalling Equation (7), the liquid side heat transfer coefficient can be determined by

$$h_{fluid} = \frac{1}{\left[\frac{1}{U\times A} - \frac{1}{(\eta^*\times h_{air}\times A_{air})}\right]\times A_{\text{fluid}}}. \tag{14}$$

6 RESULTS AND DISCUSSION

6.1 Pressure drop

Experimental measurements of the isothermal pressure drop were carried out with water and PCE-10 at 10°C. The volume flow rate through the coil was varied between 24 and 120 L/h at intervals of 8 L/h to obtain the pressure drop changes. The results are shown in Table 3 and Figure 4. For comparison, the predicted pressure drops of PCE-10 and water from numerical study were also plotted in Figure 4. The fitting formula for PCE-10 we derived by NLSF method:

$$\Delta P = 0.314\times \text{V} + 5.75. \tag{15}$$

The diagram indicated that the pressure drop of PCE-10 increased almost linearly with the flow rate, while pressure drop for water kept stable ~3.0 kPa. Pressure drop for PCE-10 was always higher than that of water, especially at higher flow rate. The extensively high pressure drop of PCE-10 was due to its high viscosity. Presence of a secondary phase dissipates kinetic energy, thus increasing the resistance to flow.

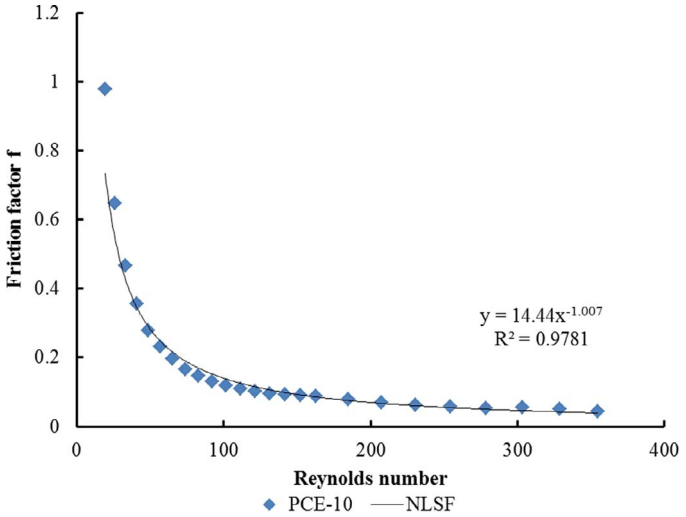

Figure 5. *Friction factor of PCME vs. Re at 10°C.*

6.2 Friction factor

In order to analytically calculate the pressure drop, the equivalent length method was adopted [27]. In this method, the equivalent length of a straight pipe, corresponding to a specific fitting (e.g. bends and manifolds) is determined. The equivalent length of a fitting is the length of a straight pipe that produces the same pressure drop as the fittings. When the equivalent length is obtained, it is added to the total pipe length and the new length is then used to calculate the pressure loss with Darcy–Weisbach formula (Equation 16).

$$\Delta P = \Delta P_s + \Delta P_{fitting} = f\frac{L}{D}\frac{\rho v^2}{2} + f\frac{L_{equ}}{D}\frac{\rho v^2}{2}, \qquad (16)$$

where

L/D = length factor, which is the ratio of the length to diameter of the pipe;

ρ = density of the fluid (kg/m3);

v = mean velocity of the flow (m/s);

f = friction actor.

The tests with water were used to determine an equivalent length of the coil bends and manifolds. Water flow at 0.1–0.5 m/s mainly fell in the laminar region. The friction factor for laminar flow can be calculated by

$$f_L = \frac{64}{\mathrm{Re}}. \qquad (17)$$

For this specified coiled pipe, the mean equivalent length corresponding to the bends and manifolds was 31 m.

Assuming the equivalent length obtained for bends and manifolds is also applicable to PCME; then, the friction factors could be determined from the experimental pressure drop measurements using Equation (16). The experimental friction factors are plotted against Re in Figure 5. The fitting formulas are derived by NLSF method:

$$f = 14.144Re^{-1.007} \quad for \quad T = 10°\mathrm{C}. \qquad (18)$$

Table 4. *Operating conditions.*

Parameter	Operating conditions
PCME volume flow rate (L/h)	144–40
Inlet air temperature(°C)	27–28
Inlet air velocity(m/s)	0.8, 1, 1.5
Inlet PCME temperature (°C)	7–8

6.3 Heat transfer

The operating conditions considered to carry out the fan-coil heat transfer tests are listed in Table 4. The experimental data shown in this section were recorded after all parameters were stable for at least 5 min.

Figure 6 shows the experimental results of the fan coil heat transfer rate against the inlet flow velocity. Analysis of the results shows that PCE-10 did help to improve the heat transfer rate by a factor of 1.1 at a constant heat transfer coefficient on average. For example, at v_{air} = 1.5 m/s, the total heat transferred by PCE-10 was about 1.1–1.2 times the value for water at the same flow rate. The same trends were witnessed in the other two cases.

The relationships between pumping power against heat transfer rate are also plotted in Figure 6. It was observed that for the same heat transfer rate, the pumping power was decreased in comparison with water. The advantage over water became more obvious at higher flow velocity.

Figure 7 demonstrates the variation of fluid-side heat transfer coefficient under different boundary conditions. The fluid side heat transfer coefficient increased with the flow velocity. It is noticed that even though the increasing air-side flow rate helped to increase the heat transfer rate, but the heat transfer coefficients did not vary significantly.

For fully developed internal laminar flow, the Nusselt numbers are constant values that depend on the hydraulic diameter.

$$Nu = \frac{hD}{k}. \qquad (19)$$

However, the above equation is only valid for straight pipes. Therefore, for coiled pipes, it is of great necessity to derive another equation. For laminar PCME, the following dimensionless parameters are used to account for the effect of PCM particles under laminar flow conditions: average Re, average Prandtl number and Stefan number [29]. A linear model was proposed based on the heat transfer coefficient data [28]:

$$Nu = 1.26\ \mathrm{Re}^{0.4}\mathrm{Pr}^{0.2}Ste^{-0.01} + 6.5 \qquad (20)$$

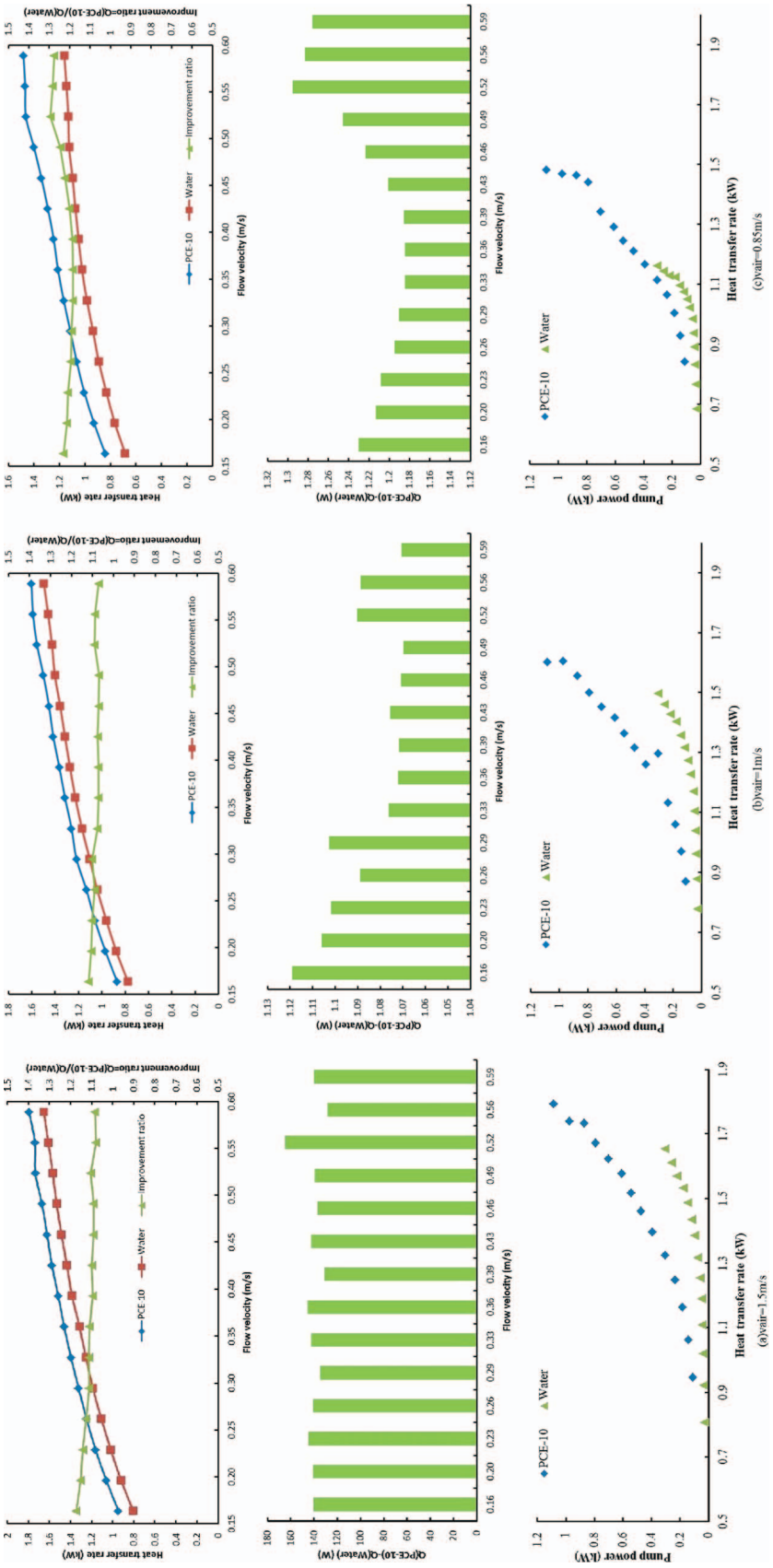

Figure 6. *Fluid side heat transfer rate vs. fluid flow velocity.*

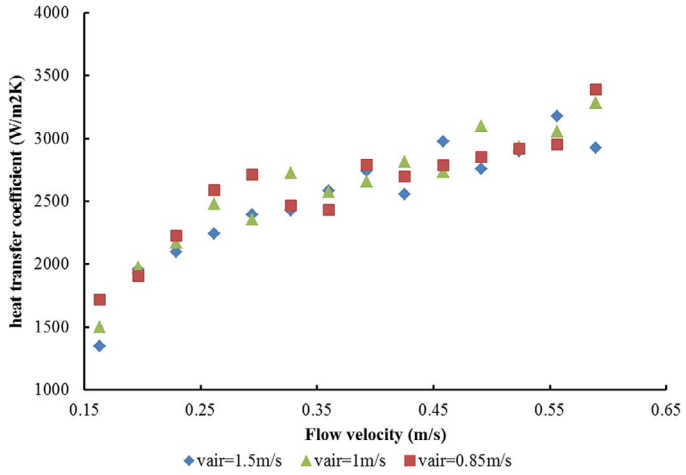

Figure 7. *Fluid side heat transfer coefficients at different boundary conditions.*

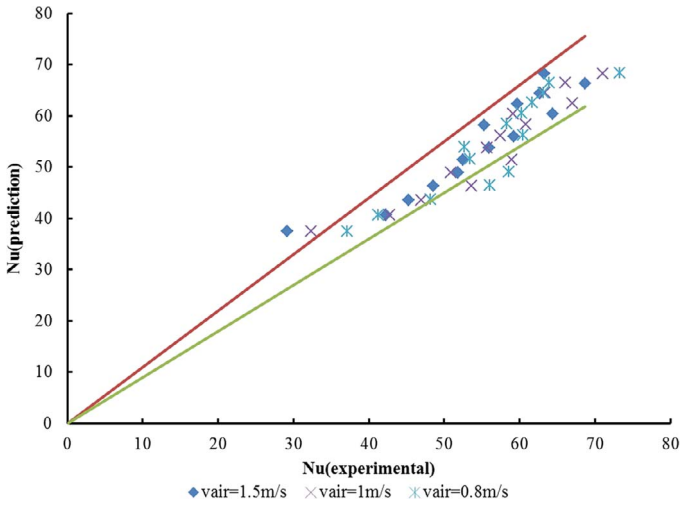

Figure 8. *Comparison of measured and predicted Nusselt number for PCME.*

$$Ste = \frac{Cp_{eff}\,\Delta T}{L} \tag{21}$$

$$\Pr = \frac{Cp_{eff}\,\mu}{k}, \tag{22}$$

where

L = latent heat,
$Cp_{,eff}$ = effective heat capacity of PCE,
ΔT = temperature difference,
K = thermal conductivity,
μ = viscosity.

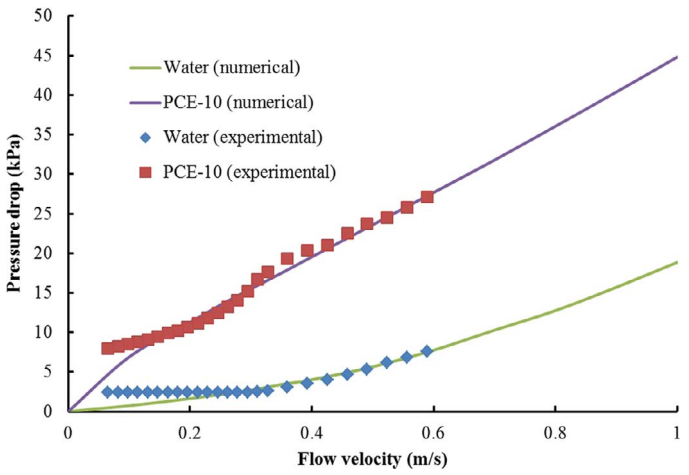

Figure 9. *Pressure drop comparison.*

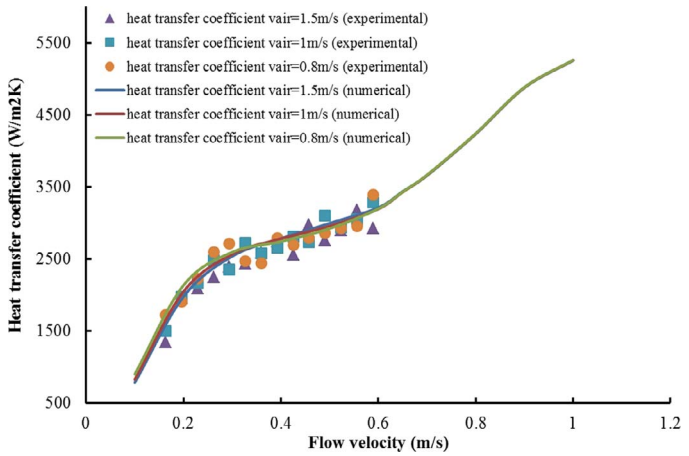

Figure 10. *Heat transfer coefficient.*

Figure 8 compares the experimental heat transfer results with those predicted by Equation (21). All the data can be predicted with Equation (21) with a standard deviation within ±10%.

6.4 Comparison with numerical results

The pressure drop and heat transfer coefficient of developed PCE-10 and water were recorded and compared with the numerical results in [23].

First of all, there was the need to ensure that the simulation and experiments were carried out at the same boundary conditions. Table 5 compares the simulation boundary conditions and

Table 5. *Experiment and simulation settings.*

	Air temperature	Air heat transfer coefficient	Fluid inlet temperature
Experimental settings	27°C–28°C	38.7, 49.9, 59.3 W/m^{2}K	7°C–8°C
Simulation settings	27°C	40, 50, 60 W/m^{2}K	7°C

experimental settings. It is safe to say the simulation and experiments were performed under similar conditions, and therefore, the results obtained were regarded as comparable.

Figure 9 compares the pressure drop for both the experimental and the numerical results. Generally, the experimental result displayed similar trend as the numerical profile. But, at low flow rate (<0.2 m/s), CFD tended to underestimate the pressure drop caused by fluid.

Figure 10 shows the heat transfer coefficients of PCE-10 under different boundary conditions. The predicted values were in good agreement with that of the experiments. The differences in heat transfer coefficient number were all within ±10%. In general, the errors were within an acceptable range and the results agreed well with the numerical predictions.

7 CONCLUSION

The flow behavior and heat transfer performance of PCME in fin-and-tube heat exchangers were evaluated experimentally. The results were used to validate the numerical prediction. The errors were within an acceptable range and the results agreed well with the numerical predictions.

The rheological performance of PCME in a coiled pipe was characterized by pressure drop across the test section. Measured pressure drop for PCE-10 was three to six times of that for water. The pressure drop for emulsion increased significantly with increasing in flow velocity. The friction factor for PCE-10 was determined by equivalent length method and the correlation between friction factor and Re have been proposed.

Thermal performance of PCE-10 in FCU was evaluated under different air flow velocities and the results were compared with water and the result suggested that PCME did help to improve the heat transfer rate of heat exchanger by factor of 1.1–1.3 at the same flow rate compared with water. Relationships between Nusselt number and Re in serpentine coiled pipes have been proposed for further studies.

In the present study, the focus is on the application in air conditioning system where the PCME flow fell in the laminar regime. But in some other possible application areas such as waste heat recovery from a heat and steam generator, the flow velocity will be higher and flow is likely be turbulent. Therefore, studies into PCME flow at higher Res are also recommended.

DATA AVAILABILITY

The data that support the findings of this study are available upon reasonable request from the authors.

FUNDING

This work was supported by the Zhejiang Provincial Natural Science Foundation of China (LQ19E080004).

REFERENCES

[1] Zhong W. 2004. Building air conditioning energy consumption and energy saving measures in China. In *Environment Engineering*. MSc Chongqing University.
[2] BSRIA. Analysis report for central air conditioning system product and its development in China. *HVACR Inf* 2014;**2**:61–74.
[3] Youssef Z, Delahaye A, Huang L *et al.* State of the art on phase change material slurries. *Energy Convers Manag* 2013;**65**:120–32.
[4] Delgado M, Lázaro A, Mazo J *et al.* Review on phase change material emulsions and microencapsulated phase change material slurries: materials, heat transfer studies and applications. *Renew Sust Energ Rev* 2012;**16**:253–73.
[5] Shao J, Darkwa J, Kokogiannakis G. Review of phase change emulsions (PCMEs) and their applications in HVAC systems. *Energy Build* 2015;**94**:200–17.
[6] Schalbart P, Kawaji M, Fumoto K. Formation of tetradecane nanoemulsion by low-energy emulsification methods. *Int J Refrig* 2010;**33**:1612–24.
[7] Huang L, Günther E, Doetsch C *et al.* Subcooling in PCM emulsions—part 1: experimental. *Thermochim Acta* 2010;**509**:93–9.
[8] Shao J, Darkwa J, Kokogiannakis G. Development of a novel phase change material emulsion for cooling systems. *Renew Energy* 2016;**87**:509–16.
[9] Morimoto T, Togashi K, Kumano H *et al.* Thermophysical properties of phase change emulsions prepared by D-phase emulsification. *Energy Convers Manag* 2016;**122**:215–22.
[10] Chen J, Zhang P. Preparation and characterization of nano-sized phase change emulsions as thermal energy storage and transport media. *Appl Energy* 2017;**190**:868–79.
[11] Kawanami T, Togashi K, Fumoto K *et al.* Thermophysical properties and thermal characteristics of phase change emulsion for thermal energy storage media. *Energy* 2016;**117**:562–8.
[12] Roy SK, Avanic BL. Turbulent heat transfer with phase change material suspensions. *Int J Heat Mass Transf* 2001;**444**:2277–85.
[13] Morimoto T, Kumano H. Flow and heat transfer characteristics of phase change emulsions in a circular tube: part 1. Laminar flow. *Int J Heat Mass Transf* 2018;**117**:887–95.
[14] Chen B, Wang X, Zhang Y *et al.* Experimental research on laminar flow performance of phase change emulsion. *Appl Therm Eng* 2006;**26**:1238–45.
[15] Morimoto T, Sugiyama M, Kumano H. Experimental study of heat transfer characteristics of phase change material emulsions in a horizontal circular tube. *Appl Therm Eng* 2021;**188**:116634.
[16] Ma F, Chen J, Zhang P. Experimental study of the hydraulic and thermal performances of nano-sized phase change emulsion in horizontal mini-tubes. *Energy* 2018;**149**:944–53.
[17] Fischer L, Maranda S, Stamatiou A *et al.* Experimental investigation on heat transfer with a phase change dispersion. *Appl Therm Eng* 2019;**147**:61–73.
[18] Vasile V, Necula H, Badea A *et al.* Experimental study of the heat transfer characteristics of a paraffin-in-water emulsion used as a secondary refrigerant. *Int J Refrig* 2018;**88**:1–7.
[19] Inaba H, Dai C, Horibe A. Natural convection heat transfer of microemulsion phase-change-material slurry in rectangular cavities heated from below and cooled from above. *Int J Heat Mass Transf* 2003;**46**:4427–38.
[20] Inaba H, Morita S. Cold heat-release characteristics of phase-change emulsion by air-emulsion direct-contact heat exchange method. *Int J Heat Mass Transf* 1996;**39**:1797–803.
[21] Zhao Z, Shi Y, Zhang Y *et al.* Flow and heat transfer characteristics of phase-change emulsion in a coiled double-tube heat exchanger. *J Eng Thermophys* 2002;**23**:730–2.
[22] Inaba H, Morita S. Flow and cold heat-storage characteristics of phase change emulsion in a coiled double tube heat exchanger. *Trans ASME* 1995;**117**:440–6.
[23] Shao J, Darkwa J, Zhang X. Numerical investigations into thermal performance of phase change emulsion in a fin-and-tube heat exchanger. *Int J Low-Carbon Technol* 2021;**16**:998–1007.

[24] Cengel YA, Turner R, Cimbala J. *Fundamentals of Thermal-fluid Sciences*4th edn. London: McGraw Hill Higher Education, 2012.
[25] Ma X, Ding G, Zhang Y *et al.* Airside heat transfer and friction characteristics for enhanced fin-and-tube heat exchanger with hydrophilic coating under wet conditions. *Int J Refrig* 2007;**30**:1153–67.
[26] Wang C, Tsai Y, Lu D. Comprehensive study of convex-louver and wavy fin-and-tube heat exchangers. *J Thermophys Heat Transf* 1998;**12**: 423–30.
[27] Yao W. *Experimental research on flow resistance characteristic in horizontal serpentine tube*. MSc Shandong University of Technology, 2011.